

Pion, Kaon and Antiproton Production in $Pb + Pb$ Collisions at LHC Energy $\sqrt{s_{NN}} = 2.76$ TeV: A Model-Based Analysis

Pradeepta Guptaroy^{1*}, Sima Guptaroy²

¹Department of Physics, Raghunathpur College, Raghunathpur, India

²Department of Physics, Basantidevi College, Kolkata, India

Email: *gpradeepta@gmail.com, simaguptaroy@yahoo.com

Received 26 January 2015; accepted 13 February 2015; published 16 February 2015

Copyright © 2015 by authors and Scientific Research Publishing Inc.

This work is licensed under the Creative Commons Attribution International License (CC BY).

<http://creativecommons.org/licenses/by/4.0/>



Open Access

Abstract

Large Hadron Collider (LHC) had produced a vast amount of high precision data for high energy heavy ion collision. We attempt here to study i) transverse momenta spectra, ii) K/π , p/π ratio behaviours, iii) rapidity distribution, and iv) the nuclear modification factors of the pion, kaon and antiproton produced in $p + p$ and $Pb + Pb$ collisions at energy $\sqrt{s_{NN}} = 2.76$ TeV, on the basis of Sequential Chain Model (SCM). Comparisons of the model-based results with the measured data on these observables are generally found to be modestly satisfactory.

Keywords

Relativistic Heavy Ion Collisions, Baryon Production, Light Mesons

1. Introduction

Heavy ion collisions at ultra relativistic energies might produce a new form of QCD matter characterized by the deconfined state of quarks and gluons (partons) [1]. Measurements of the production of identified particles provide information about the dynamics of this dense matter. The yield of identified hadrons, their multiplicity distributions, as well as the rapidity and transverse momentum spectra are the basic observables in proton-proton and heavy ion collisions at any energy regime, from a few GeV per nucleon to the new ultra-relativistic LHC regime, spanning c.m. energies of a few TeV [2]. Recently, the different experimental groups in the CERN

*Corresponding author.

Large Hadron Collider (LHC) have reported various results for different observables in $Pb+Pb$ collisions at energy $\sqrt{s_{NN}} = 2.76$ TeV. These results might provide another opportunity to investigate the bulk properties of exotic QCD matter, the so-called QGP-hypothesis. But the exact nature of QGP-hadron phase transition is still plagued by uncertainties [3].

Our objective in this work is to use a model, known as ‘‘Sequential Chain Model (SCM)’’, which is different from ‘‘standard’’ framework, in interpreting the transverse momenta spectra, some ratio-behaviours, rapidity spectra and the nuclear modification factor of the pions, kaons and antiprotons produced in $p+p$ and $Pb+Pb$ collisions at LHC energy $\sqrt{s_{NN}} = 2.76$ TeV. Very recently, some questions have been arose about the quark constituents of the nucleons. Little of the proton spin is carried by the quarks [4]. So, in order to explain the huge amount of heavy ion collision data, we put forward this model which has no QGP-tag and is different from the quark-hypothesis.

The organization of this work is as follows. In Section 2, we give a brief outline of our approach, the SCM. In the next section (Section 3), the results have been presented with table and figures. And in the last section (Section 4), we offer the final remarks and conclusions.

2. Outline of the Model

This section is divided by two subsections 1) the basic model in $p+p$ collision and 2) subsequent transformation to the $A+B$ collisions.

2.1. The Basic Model: An Outline

According to this Sequential Chain Model (SCM), high energy hadronic interactions boil down, essentially, to the pion-pion interactions; as the protons are conceived in this model as $p = (\pi^+ \pi^0 \mathcal{G})$, where \mathcal{G} is a spectator particle needed for the dynamical generation of quantum numbers of the nucleons [5]-[11].

The inclusive cross-section of the π^- -meson produced in the $p+p$ collisions at high energies has been calculated by using field theoretical calculations and Feynman diagram techniques with the infinite momentum frame approximation method. The inclusive cross-section is given by the undernoted relation [5]-[11]

$$E \frac{d^3\sigma}{dp^3} \Big|_{pp \rightarrow \pi^- x} \cong \Gamma_{\pi^-} \exp\left(-2.38 \langle n_{\pi^-} \rangle_{pp} x\right) \frac{1}{p_T^{(N_R^-)}} \exp\left(\frac{-2.68 p_T^2}{\langle n_{\pi^-} \rangle_{pp} (1-x)}\right) \quad (1)$$

with

$$\langle n_{\pi^+} \rangle_{pp} \cong \langle n_{\pi^-} \rangle_{pp} \cong \langle n_{\pi^0} \rangle_{pp} \cong 1.1s^{1/5} \quad (2)$$

where Γ_{π^-} is the normalisation factor which will increase as the inelastic cross-section increases and it is different for different energy and for various collisions. The terms p_T , x ,

$[x = 2p_{zcm}/\sqrt{s} = 2m_T \sin\theta_{cm}/\sqrt{s}]$ in Equation (1) represent the transverse momentum, Feynman Scaling variable respectively. The s in Equation (2) is the square of the c.m. energy.

$1/p_T^{N_R^-}$ of the expression (1) is the ‘‘constituent rearrangement term’’. It arises out of the partons inside the proton. At high energy interaction processes the partons undergo some dissipation losses due to impact and impulses of the projectile on the target. This term essentially provides a damping term in terms of a power law. The exponent of p_T , *i.e.* N_R , varies on both the collision process and the specific p_T -range. We have to parametrize this term with the view of two physical points, *viz.*, the amount of momentum transfer and the contributions from a phase factor arising out of the rearrangement of the constituent partons. The relation for N_R is to be given by [12]

$$N_R = 4 \langle N_{\text{part}} \rangle^{1/3} \theta \quad (3)$$

where $\langle N_{\text{part}} \rangle$ denotes the average number of participating nucleons and θ values are to be obtained phenomenologically from the fits to the data-points.

Similarly, for kaons of any specific variety (K^+ , K^- , K^0 or \bar{K}^0) we have

$$E \frac{d^3\sigma}{dp^3} \Big|_{pp \rightarrow K^- X} \cong \Gamma_{K^-} \exp\left(-6.55 \langle n_{K^-} \rangle_{pp} x\right) \frac{1}{p_T \left(\frac{N_{K^-}}{p_T}\right)} \exp\left(\frac{-1.33 p_T^2}{\langle n_{K^-} \rangle_{pp}^{3/2}}\right) \quad (4)$$

with

$$\langle n_{K^+} \rangle_{pp} \cong \langle n_{K^-} \rangle_{pp} \cong \langle n_{K^0} \rangle_{pp} \cong \langle n_{\bar{K}^0} \rangle_{pp} \cong 5 \times 10^{-2} s^{1/4} \quad (5)$$

And for the antiproton production in pp collision at high energies, the derived expression for inclusive cross-section is

$$E \frac{d^3\sigma}{dp^3} \Big|_{pp \rightarrow \bar{p} X} \cong \Gamma_{\bar{p}} \exp\left(-25.4 \langle n_{\bar{p}} \rangle_{pp} x\right) \frac{1}{p_T \left(\frac{N_{\bar{p}}}{p_T}\right)} \exp\left(\frac{-0.66 \left(\left(\frac{p_T^2}{p}\right) + m_{\bar{p}}^2\right)}{\langle n_{\bar{p}} \rangle_{pp}^{3/2} (1-x)}\right) \quad (6)$$

with

$$\langle n_{\bar{p}} \rangle_{pp} \cong \langle n_p \rangle_{pp} \cong 2 \times 10^{-2} s^{1/4} \quad (7)$$

2.2. The Path from pp to AB Collisions

In order to transform the inclusive cross-section from $pp \rightarrow C^- + X$ to $AB \rightarrow C^- + X$ collisions (here, C^- stands for π^- , K^- and \bar{p} , as the case may be), we use the undernoted relation [13];

$$E \frac{d^3\sigma}{dp^3} \Big|_{AB \rightarrow C^- + X} \cong \frac{(A\sigma_B + B\sigma_A)}{\sigma_{AB}} \frac{1}{1 + a'(A^{1/3} + B^{1/3})} E \frac{d^3\sigma}{dp^3} \Big|_{pp \rightarrow C^- + X} \quad (8)$$

Here, in the above equation [Equation (8)], the first factor gives a measure of the number of wounded nucleons *i.e.* of the probable number of participants, wherein $A\sigma_B$ gives the probability cross-section of collision with “ B ” nucleus (target), had all the nucleons of A suffered collisions with B -target. And $B\sigma_A$ has just the same physical meaning, with A and B replaced. Furthermore, σ_A is the nucleon (proton)-nucleus (A) interaction cross-section, σ_B is the inelastic nucleon (proton)-nucleus (B) reaction cross-section and σ_{AB} is the inelastic AB cross-section for the collision of nucleus A and nucleus B . The values of σ_{AB} , σ_A , σ_B have been worked here out by the following formula [14]

$$\sigma_{AB}^{\text{inel}} = \sigma_0 \left(A_{\text{projectile}}^{1/3} + A_{\text{target}}^{1/3} - \delta \right)^2 \quad (9)$$

with $\sigma_0 = 68.8$ mb, $\delta = 1.32$.

The second term in expression (8) is a physical factor related with energy degradation of the secondaries due to multiple collision effects. The parameter a' occurring in this term is a measure of the fraction of the nucleons that suffer energy loss. The maximum value of a' is unity, while all the nucleons suffer energy loss. This a' parameter is usually to be chosen [13], depending on the centrality of the collisions and the nature of the secondaries.

3. The Results

This section will be divided in the following sub-sections: i) the p_T -spectra of pion, kaon and antiproton in both $p+p$ and $Pb+Pb$ collisions at $\sqrt{s_{NN}} = 2.76$ TeV; ii) K/π and p/π ratio behaviour at $Pb+Pb$ collisions at $\sqrt{s_{NN}} = 2.76$ TeV; iii) rapidity distribution of pion for the most central collisions of $Pb+Pb$ in the above-mentioned energy and iv) the nuclear modification factor R_{AA} in the same energy range.

3.1. Transverse Momenta Spectra of Charged Hadron in $p+p$ and $Pb+Pb$ Collision at $\sqrt{s_{NN}} = 2.76$ TeV

We can write from expression (8), the transformed SCM-based transverse-momentum distributions for $A+B \rightarrow C^- + X$ -type reactions in the following generalized notation:

$$\frac{1}{2\pi p_T} \frac{d^2 N}{dp_T dy} \Big|_{A+B \rightarrow C^- + x} = \alpha_{C^-} \frac{1}{p_T^{N_R^{C^-}}} \exp(-\beta_{C^-} \times p_T^2) \quad (10)$$

where, for example, the parameter α_{π^-} can be written in the following form:

$$\alpha_{\pi^-} = \frac{(A\sigma_B + B\sigma_A)}{\sigma_{AB}} \frac{1}{1 + a(A^{1/3} + B^{1/3})} \Gamma_{\pi^-} \exp\left(-2.38 \langle n_{\pi^-} \rangle_{pp} x\right) \quad (11)$$

In a similar way, the values of β_{π^-} of Equation (10) have been calculated with the help of Equation (1), Equation (2). The values of α_{K^-} , $\alpha_{\bar{p}}$, β_{π^-} and $\beta_{\bar{p}}$ have been calculated accordingly by using Equations (4)-(8). Moreover, for calculation for transverse momenta distribution of antiproton production, the the exponential part will be $\exp(-\beta_{\bar{p}}(p_T^2 + m_{\bar{p}}^2))$ ($m_{\bar{p}} \sim 938 \text{ MeV}/c^2$).

$N_R^{C^-}$ of the expression (10) have been calculated by using Equation (3).

3.1.1. Production of π^- , K^- and \bar{p} in $p+p$ Collision at $\sqrt{s_{NN}} = 2.76 \text{ TeV}$

In **Table 1**, the calculated values of α , N_R and β of Equation (10) for π^- , K^- and \bar{p} produced in proton-proton collisions at $\sqrt{s_{NN}} = 2.76 \text{ TeV}$ have been given.

In **Figure 1**, we have drawn the invariant yields against p_T for π^- , K^- and \bar{p} . By using Equation (10) and **Table 1** we have plotted the solid lines against the experimental background [15]. The dotted lines in the figure show PYTHIA-based results [15].

3.1.2. Invariant Yields of π^- , K^- and \bar{p} in $Pb+Pb$ Collision at $\sqrt{s_{NN}} = 2.76 \text{ TeV}$

In a similar fashion, the invariant yields of π^- , K^- and \bar{p} in $Pb+Pb$ collision at LHC energy $\sqrt{s_{NN}} = 2.76 \text{ TeV}$ for different centralities have been plotted in **Figures 2(a)-(c)** respectively. The solid lines in the figure are the theoretical SCM results while the points show the experimental values [16]. The values of α_{C^-} , $N_R^{C^-}$ and β_{C^-} of Equation (10) for pion, kaon and antiproton and for different centralities have been given in **Table 2**.

3.2. The K/π and p/π Ratios

The model-based K/π and p/π ratios as a function of p_T at energies $\sqrt{s_{NN}} = 2.76 \text{ TeV}$ have been obtained from the expression (10) and **Table 2**. Data in **Figure 3(a)** and **Figure 3(b)**, for different centralities, viz., for 0% - 5%, 20% - 30% and 70% - 80%, are taken from Ref [16]. Lines in the figure show the theoretical plots.

3.3. The Rapidity Distribution

For the calculation of rapidity distribution, we can make use of the following standard relation [17],

$$\frac{dN}{dy} = \frac{1}{\sigma_{in}} \int \left[E \frac{d^3 \sigma}{dp^3} \right] d^2 p_T \quad (12)$$

Table 1. Values of α , N_R and β for pions, kaons, antiproton and proton productions in $p+p$ collisions at $\sqrt{s_{NN}} = 2.76 \text{ TeV}$.

$(\alpha_{\pi^-})_{pp}$	$(N_R^{\pi^-})_{pp}$	$(\beta_{\pi^-})_{pp}$
0.581	2.163	0.30
$(\alpha_{K^-})_{pp}$	$(N_R^{K^-})_{pp}$	$(\beta_{K^-})_{pp}$
0.165	1.454	0.180
$(\alpha_{\bar{p}})_{pp}$	$(N_R^{\bar{p}})_{pp}$	$(\beta_{\bar{p}})_{pp}$
0.105	1.573	0.180

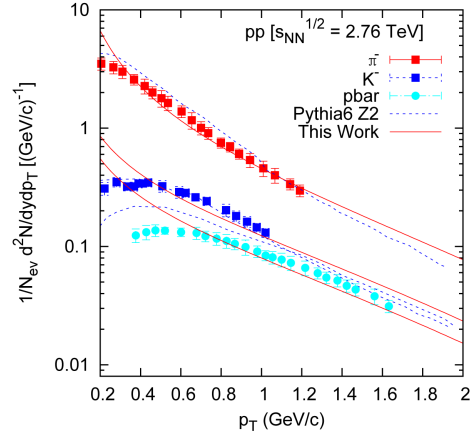


Figure 1. Plots for π^- , K^- , \bar{p} and p productions in $p + p$ collisions at energies $\sqrt{s_{NN}} = 2.76$ TeV. Data are taken [15]. Solid lines in the figures show the SCM-based theoretical plots while the dotted ones show PYTHIA-based results [15].

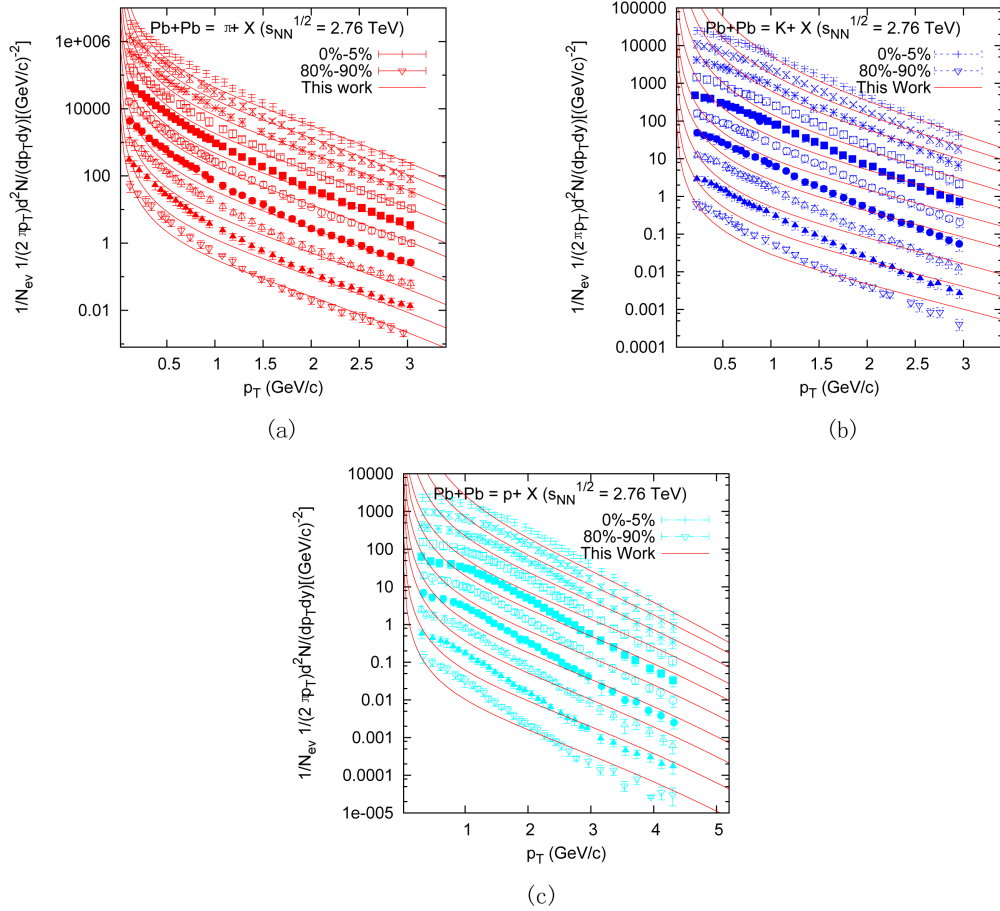


Figure 2. Centrality dependence of the p_T distribution for (a) π^- , (b) K^- and (c) \bar{p} for different centralities in $Pb + Pb$ collisions at energies $\sqrt{s_{NN}} = 2.76$ TeV. Data are taken from [16]. The solid lines in the (a)-(c) show the SCM calculations for different centralities.

Table 2. Values of $(\alpha)_{PbPb}$, $(N_R)_{PbPb}$ and $(\beta)_{PbPb}$ for different centralities for the π^- , K^- and \bar{p} productions in $Pb + Pb$ collisions at $\sqrt{s_{NN}} = 2.76$ TeV.

Centrality	$(\alpha_{\pi^-})_{PbPb}$	$(N_R^{\pi^-})_{PbPb}$	$(\beta_{\pi^-})_{PbPb}$
0% - 5%	5.8×10^4	2.493	0.30
5% - 10%	2.5×10^4	2.483	0.30
10% - 20%	8.5×10^3	2.472	0.30
20% - 30%	2.5×10^3	2.464	0.30
30% - 40%	6.8×10^2	2.456	0.30
40% - 50%	2.5×10^2	2.444	0.30
50% - 60%	48	2.434	0.30
60% - 70%	9.1	2.415	0.30
70% - 80%	1.8	2.397	0.30
80% - 90%	0.45	2.392	0.30
Centrality	$(\alpha_{K^-})_{PbPb}$	$(N_R^{K^-})_{PbPb}$	$(\beta_{K^-})_{PbPb}$
0% - 5%	6.3×10^3	3.314	0.180
5% - 10%	3.1×10^3	3.015	0.180
10% - 20%	7.4×10^2	2.784	0.180
20% - 30%	1.8×10^2	2.583	0.180
30% - 40%	46	2.321	0.180
40% - 50%	12	2.124	0.180
50% - 60%	3.2	2.111	0.180
60% - 70%	0.62	2.104	0.180
70% - 80%	0.14	2.008	0.180
80% - 90%	0.034	1.984	0.180
Centrality	$(\alpha_{\bar{p}})_{PbPb}$	$(N_R^{\bar{p}})_{PbPb}$	$(\beta_{\bar{p}})_{PbPb}$
0% - 5%	3.1×10^3	3.114	0.180
5% - 10%	8.4×10^2	2.723	0.180
10% - 20%	2.6×10^2	2.534	0.180
20% - 30%	66	2.302	0.180
30% - 40%	23	2.286	0.180
40% - 50%	5.9	2.234	0.180
50% - 60%	1.5	2.201	0.180
60% - 70%	0.43	2.194	0.180
70% - 80%	0.072	2.075	0.180
80% - 90%	0.012	2.034	0.180

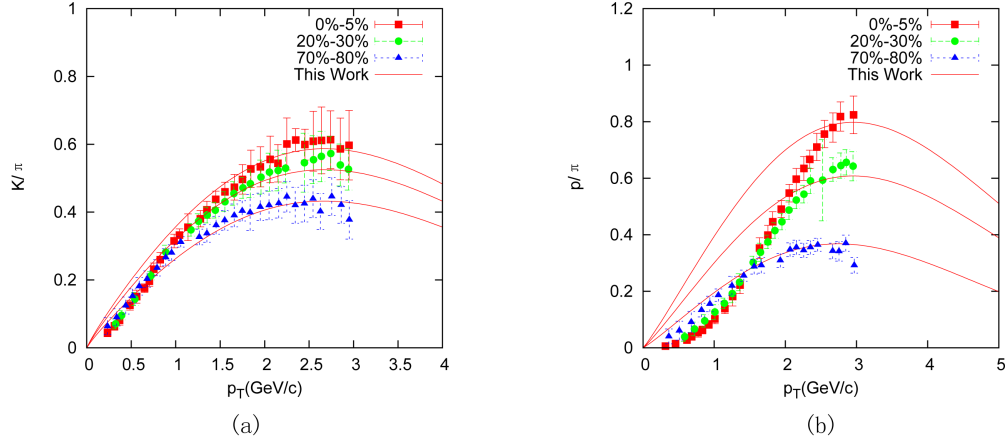


Figure 3. Ratios of (a) K/π and (b) p/π as a function p_T for 0% - 5%, 20% - 30% and 70% - 80% $Pb+Pb$ reactions at $\sqrt{s_{NN}} = 2.76$ TeV. Data in these figures are taken from [16]. The solid lines show the SCM-based results.

By using Equation (1), Equation (8), **Table 2** and Equation (12), we arrive at the SCM-based rapidity distribution, which is given hereunder;

$$\frac{dN}{dy} = 1895 \exp(-0.025 \sinh y_{cm}) \quad (13)$$

The y_{cm} of the above equation (Equation (13)) has come from $\exp(-2.38 \langle n_{\pi^-} \rangle x)$ of Equation (11) with $x = 2m_T \sinh y_{cm} / \sqrt{s}$.

In **Figure 4**, we have plotted theoretical dN/dy versus y with the help of above equation [Equation (13)] against experimental background [18]. The dotted line in this figure shows the Gaussian fit [18].

3.4. The Nuclear Modification Factor

The nuclear modification factor (NMF) R_{AA} is defined as ratio of charged particle yield in $Pb+Pb$ to that in $p+p$, scaled by the number of binary nuclear collisions $\langle N_{coll} \rangle$ [19] and is given hereunder

$$R_{AA}(p_T) = \frac{(1/N_{evt}^{AA}) d^2 N_{ch}^{AA} / dp_T d\eta}{\langle N_{coll} \rangle (1/N_{evt}^{pp}) d^2 N_{ch}^{pp} / dp_T d\eta} \quad (14)$$

where $\langle N_{coll} \rangle$ is related with the average nuclei thickness function $\langle \langle T_{AA} \rangle \rangle$ by the following relation [19]

$$\langle N_{coll} \rangle = \langle T_{AA} \rangle \sigma_{pp}^{incl} \quad (15)$$

Here, σ_{pp}^{incl} is the total inelastic cross section of $p+p$ interactions.

The $d^2 N / dp_T d\eta$ is related to $d^2 N / dp_T dy$ by the following relation [13]:

$$\frac{d^2 N}{dp_T d\eta} = \sqrt{1 - \frac{m^2}{m_T^2 \cosh^2 y}} \frac{d^2 N}{dp_T dy} \quad (16)$$

In the region, $y \gg 0$, $\frac{d^2 N}{dp_T d\eta} \sim \frac{d^2 N}{dp_T dy}$.

The SCM-based results on NMF's for π^- , K^- and \bar{p} in central $Pb+Pb$ collisions at energies $\sqrt{s_{NN}} = 2.76$ TeV are deduced on the basis of Equation (10), **Table 1** and **Table 2**. The equations in connection with $(R_{AA})_{\pi^-}$, $(R_{AA})_{K^-}$ and $(R_{AA})_{\bar{p}}$ are give by the following relations and they are plotted in **Figure 5** against p_T . The solid lines in the figure show the theoretical results, while the points show the experimentally measured results [20];

$$(R_{AA})_{\pi^-} = 0.35 p_T^{0.33} \quad (17)$$

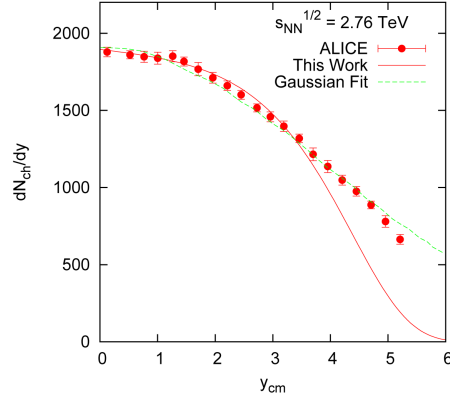


Figure 4. Plot of rapidity distribution of π in central $Pb+Pb$ reactions at $\sqrt{s_{NN}} = 2.76$ TeV. Data in the figure are taken from [18]. The solid line shows the SCM-based results while the dotted line depicts the Gaussian fit [18].

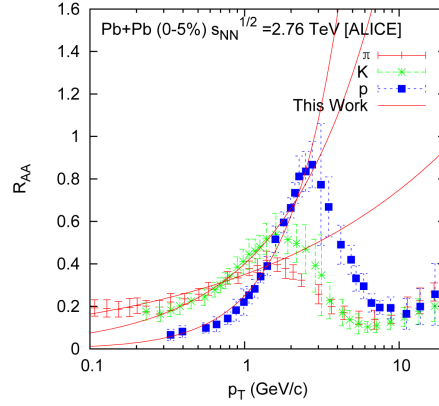


Figure 5. Plots for R_{AA} versus p_T in central $Pb+Pb$ collisions at energies $\sqrt{s_{NN}} = 2.76$ TeV. Data are taken from Ref [20]. Solid lines in the figure show the SCM-based theoretical plots.

$$(R_{AA})_{K^-} = 0.40 p_T^{0.73} \quad (18)$$

$$(R_{AA})_{\bar{p}} = 0.25 p_T^{1.33} \quad (19)$$

4. Discussions and Conclusions

Let us now make some comments on the results arrived at and shown by the diagrams on the case-to-case basis.

1) The invariant yields against transverse momenta (p_T) for π^- , K^- and \bar{p} in proton-proton collisions obtained on the basis of the SCM are shown in **Figure 1**. Except for very low- p_T region, there is a bit degree of success. The model disagrees in the low- p_T region. This is due to the fact that the model has turned essentially into a mixed one with the inclusion of power law due to the inclusion of partonic rearrangement factor. However, the power-law part of the equation might not be the only factor for this type of discrepancy. The initial condition and dynamical evolution in heavy-ion collisions are more complicated than we expect. Till now, we do not know the exact nature of reaction mechanism. One might take into account some other factors like radial flow or thermal equilibrium.

2) Similarly, in calculating the yields for different transverse momenta and for different centralities for π^- , K^- and \bar{p} in lead-lead collisions, we use Equations (8), (9) and (10) along with Equations (1)-(7). The results

are given in **Table 2** and are depicted in **Figures 2(a)-(c)** respectively. The top-most curves are for central collisions (0% - 5%) and the lowest curves are peripheral ones (80% - 90%). In between these two curves, other centralities (5% - 10%, 10% - 20%, 20% - 30%, 30% - 40%, 40% - 50%, 50% - 60%, 60% - 70% and 70% - 80%) have been plotted. For the production of pions, the SCM-based results show good fits from central to peripheral collision. Slight disagreements observed at very low- p_T regions for kaons and protons at central collisions. These are due to the power law part of the model. This explanation is also true for low- p_T region data in $p + p$ collision. Here, we see that the constituent rearrangement terms are clearly centrality dependent.

3) The K/π and p/π ratio behaviours for different centralities are calculated in the light of the SCM and they are plotted in **Figure 3(a)** and **Figure 3(b)** respectively. The theoretical K/π ratio behaviours are in good agreement with experimental values. Some disagreement are observed in central p/π -ratio in low- p_T regions.

4) In explaining the rapidity distribution for production of pions (**Figure 4**), the majority of the produced secondaries, the model works agreeably with data. The comparison with Gaussian fit is satisfactory.

5) The nuclear modification factors for pion, kaon and proton for central $Pb + Pb$ collisions for different transverse momenta have been calculated and they are plotted in **Figure 5**. While the theoretical plots are agreeable in low- p_T regions, they disagree in high- p_T .

Now, let us sum up our observations in the following points: 1) The model under consideration here explains the data modesly well on $Pb + Pb$ collisions at $\sqrt{s_{NN}} = 2.76$ TeV. 2) The particle production in heavy ion collisions can be viewed alternatively by this Sequential Chain Model.

Acknowledgements

The work is supported by University Grants Commission, India, against the order no. PSW-30/12(ERO) dt.05 Feb-13.

References

- [1] Abelev, B. [ALICE Collaboration] (2014) *Physics Letters B*, **736**, 196-207.
<http://dx.doi.org/10.1016/j.physletb.2014.07.011>
- [2] Riggi, F. (2013) *Journal of Physics: Conference Series*, **424**, Article ID: 012004.
<http://dx.doi.org/10.1088/1742-6596/424/1/012004>
- [3] Zhang, S., Han, L.X., Ma, Y.G., Chen, J.H. and Zhong, C. (2014) *Physical Review C*, **89**, Article ID: 034918.
<http://dx.doi.org/10.1103/PhysRevC.89.034918>
- [4] de Florian, D., Sassot, R., Stratmann, M. and Vogelsang, W. (2014) *Physical Review Letters*, **113**, Article ID: 012001.
<http://dx.doi.org/10.1103/PhysRevLett.113.012001>
- [5] Guptaroy, P. and Guptaroy, S. (2014) *Chinese Physics Letters*, **31**, Article ID: 082501.
<http://dx.doi.org/10.1088/0256-307X/31/8/082501>
- [6] Guptaroy, P., Goutam, S. and Bhattacharyya, S. (2012) *Journal of Modern Physics*, **3**, 116-123.
<http://dx.doi.org/10.4236/jmp.2012.31016>
- [7] Guptaroy, P., Sau, G., Biswas, S.K. and Bhattacharyya, S. (2010) *IL Nuovo Cimento B*, **125**, 1071-1097.
<http://dx.doi.org/10.1393/ncb/i2010-10913-4>
- [8] Guptaroy, P., De Bhaskar, Sau, G., Biswas, S.K. and Bhattacharyya, S. (2007) *International Journal of Modern Physics A*, **28**, 5121-5154. <http://dx.doi.org/10.1142/S0217751X07037251>
- [9] Bandyopadhyay, P. and Bhattacharyya, S. (1978) *IL Nuovo Cimento A*, **43**, 305-322.
<http://dx.doi.org/10.1007/BF02730432>
- [10] Bhattacharyya, S. (1988) *IL Nuovo Cimento C*, **11**, 51-65. <http://dx.doi.org/10.1007/BF02507895>
- [11] Bhattacharyya, S. (1988) *Journal of Physics G: Nuclear Physics*, **14**, 9-17.
<http://dx.doi.org/10.1088/0305-4616/14/1/005>
- [12] Guptaroy, P., Sau, G., Biswas, S.K. and Bhattacharyya, S. (2008) *Modern Physics Letters A*, **23**, 1031-1046.
<http://dx.doi.org/10.1142/S021773230802567X>
- [13] Wong, C.Y. (1994) *Introduction to High-Energy Heavy Ion Collisions*. World Scientific, Singapore.
<http://dx.doi.org/10.1142/9789814277549>
- [14] Abreu, M.C., Alessandro, B., Alexa, C., Arnaldi, R., Atayan, M., Baglin, C., *et al.* (2002) *Physics Letters B*, **530**, 33-42.
[http://dx.doi.org/10.1016/S0370-2693\(02\)01352-7](http://dx.doi.org/10.1016/S0370-2693(02)01352-7)

- [15] Chatrchyan, S., Khachatryan, V., Sirunyan, A.M., Tumasyan, A., Adam, W., Aguilo, E., *et al.*, the CMS Collaboration (2012) *The European Physical Journal C*, **72**, 2164. <http://dx.doi.org/10.1140/epjc/s10052-012-2164-1>
- [16] Abelev, B., Adam, J., Adamová, D., Adare, A.M., Aggarwal, M.M., Aglieri Rinella, G., *et al.* (2013) *Physical Review C*, **88**, Article ID: 044910. <http://dx.doi.org/10.1103/PhysRevC.88.044910>
- [17] Kaidalov, A.B. and Ter-Martirosyan, K.A. (1984) *Soviet Journal of Nuclear Physics*, **39**, 979.
- [18] ALICE Collaboration (2013) *Physics Letters B*, **726**, 610-622. <http://dx.doi.org/10.1016/j.physletb.2013.09.022>
- [19] Otwinowski, J. (2013) High- p_T Processes Measured with ALICE at the LHC. arXiv:1301.5285v1 [hep-ex]
- [20] Chojnacki, M., for the ALICE Collaboration (2014) *Journal of Physics: Conference Series*, **509**, Article ID: 012041. <http://dx.doi.org/10.1088/1742-6596/509/1/012041>

Scientific Research Publishing (SCIRP) is one of the largest Open Access journal publishers. It is currently publishing more than 200 open access, online, peer-reviewed journals covering a wide range of academic disciplines. SCIRP serves the worldwide academic communities and contributes to the progress and application of science with its publication.

Other selected journals from SCIRP are listed as below. Submit your manuscript to us via either submit@scirp.org or **Online Submission Portal**.

